

Analytical solution of discontinuous contact problem in functionally graded layer and homogeneous layer

Yusuf Kaya*¹, Alper Polat², Talat Şükrü Özşahin³, Pınar Bora⁴

¹ Department of Civil Engineering, Gumushane University, Gumushane 29100, Turkey

² Department of Civil Engineering, Munzur University, Tunceli 62000, Turkey

³ Department of Civil Engineering, Karadeniz Technical University, Trabzon 61080, Turkey

⁴ Department of Civil Engineering, Sivas Cumhuriyet University, Sivas 58140, Turkey

(Received May 13, 2023, Revised October 7, 2024, Accepted October 30, 2025)

Abstract. In the study, the problem of discontinuous contact in two layers, one of which is functionally graded is solved using the theory of elasticity. In this problem functionally graded (FG) layer resting on homogeneous layer and loaded with two different rigid flat blocks. In addition, homogeneous layer is resting on a rigid plane. Frictions on all surfaces are neglected. The heights of the FG layer and the homogeneous layer are h_1 and h_2 , respectively. When solving the problem, displacement and stress equations are substituted in the boundary conditions. Then the problem is demained to singular integral equations. Wherein unknown functions are the contact stresses under the two rigid flat blocks and the slope of the separation. These singular integral equations are solved numerically using the Gauss-Chebyshev integration formulas. The analyzes were performed for different inhomogeneity parameter (βh_1), shear modulus ratio (μ_2/μ_{-h_1}), distance between the rigid blocks ($(a_3-a_2)/h_1$) and density parameter (γh_1). Consequently, the stress distributions and starting and ending points of the separation area between the FG layer and homogeneous layer are determined for several dimensionless quantities.

Keywords: discontinuous contact problem; functionally graded layer; rigid plane; separation; theory of elasticity

1. Introduction

Various new materials have emerged depending on the changing needs with the developing technology. These are generally produced as composite materials, and many studies are carried out on the physical and mechanical properties of these materials using analytical, experimental and finite element methods. Hussain et al. [1] performed a numerical study of the nonlocal vibration of orthotropic single-walled carbon nanotubes (SWCNTs) using Kelvin's model. Singh et al. [2] performed a correlation study on the microstructure and mechanical properties of geopolymer pastes consisting of rice husk ash-Sodium aluminate. Hussain et al. investigated the effect of Young's Modulus on vibration of double-walled carbon nanotubes with elastic shell model [3]. Khan et al. [4] investigated the effect of fiber content on the performance of Ultra high performance concrete slabs under impact load experimentally and analytically. One of the newly produced composite materials is functionally graded materials. Functionally graded materials (FGM) are defined as

*Corresponding author, Ph.D., Assistant Professor, E-mail: yusufkaya@gumushane.edu.tr

heterogeneous special microstructures whose material properties change from one point to another, regularly and continuously depending on a function. Unlike the layered structures, in functionally graded (FG) materials, material properties such as density, shear modulus change functionally and continuously from one surface of the material to the other surface. Due to the graded structure in the FGMs, it minimizes the fractures, interface and surface cracks that occur because of the sudden cross section change in layered materials with different properties. Since their emergence, FGMs have found a wide range of applications, mainly in the aviation and space industries. (rocket engine parts, spacecraft body), chemical (heat exchanger, reactor boiler), biometals (implants, artificial leather), mechanical, construction (building materials), electrical circuit (semiconductors, sensors) industries. Additionally, functionally graded materials have also been the subject of work in the area of contact mechanics.

Most structures and components of mechanical systems are in contact with each other. The subject of contact mechanics was studied by Hertz firstly. Until now, several studies have been done about contact problem in homogeneous layers and FG layers. Some of these studies are: Chen and Engel discussed the contact problem of the one or two layer system loaded with a rigid block and resting on the elastic half plane [5]. Keer and Miller studied the contact problem of a curvilinear block and a circular plate resting on simple or recessed supports from its sides [6]. Geçit [7] investigated the axisymmetric contact problem of an elastic semi-infinite circular cylinder pressed against the elastic half-plane. Çakıroğlu et al. [8] investigated the continuous and DCCP of two elastic layers resting on an elastic semi-infinite plane. Yaylacı and Avcar [9] solved the continuous and discontinuous contact problem of a functionally graded (FG) layer resting on a homogeneous half-plane and loaded with a distributed load, using the finite element method and analytically. Hartmann et al. [10] studied a three-dimensional contact domain method for large deformation frictionless contact problems. Oliver et al. [11] investigated the theoretical basis of a frictional contact domain method for two-dimensional large deformation problems. Chidlow et al. [12] studied the frictionless contact problem of an inhomogeneous material loaded by a rigid block.

Güler and Erdoğan [13] have analyzed the problem of frictional contact in the elastic semi-infinite plane covered with a FG layer. El-Borgi et al. [14] discussed the frictionless and receding contact problem of a FG layer loaded with a distributed load and resting on an elastic semi-infinite plane. Elloumi et al. [15] investigated the two-dimensional nonlinear shear contact problem occurring between a FG semi-infinite plane and an arbitrary shaped block loaded with a single load. Rekik et al. [16] analyzed analytically an axis symmetrical problem of a buried crack in a FG layer bonded to a homogeneous half-plane. Nikbakht et al. [17] studied the frictionless elastic contact between a FG low carbon steel plate and a rigid spherical block. Talezadehlari et al. [18] investigated the frictional two-dimensional contact problem for rigid circular and flat blocks in case of surface cracks in the FG layer resting on the elastic semi-infinite plane. Kaya [19] solved the contact problem in a FG layer and homogeneous layer resting on a rigid plane by using elasticity theory and Fourier integral transforms. Balci and Dağ [20] analyzed analytically the dynamic frictional contact problem between FG coating and a moving rigid block. Polat [21] solved the continuous contact problem of a functionally graded (FG) layer resting on a homogeneous half-plane and loaded with a functionally graded block using the finite element method (FEM). Polat et al. [22] solved the continuous contact problem of a FG layer loaded by a rigid flat block and resting on an elastic half-plane by using the finite element method. Yan and Mi [23] investigated the receding contact problem of a homogeneous layer resting on a semi-infinite plane and reinforced with FG layer. Kaya et al. [24] solved the continuous contact problem of two layers one of which was FG, resting on a rigid plane and loaded with two rigid blocks analytically and using finite element method. Öner and Birinci [25] solved the

continuous and DCCP between a functionally graded (FG) layer symmetrically loaded by a rigid block and a homogeneous semi-infinite plane analytically. Yaylacı and Avcar [9] investigated the receding contact problem of a homogeneous layer resting on two elastic quarter planes and loaded with a circular rigid block, using the finite element method (FEM). Polat and Kaya [26] solved the discontinuous contact problem of two functional layers resting on a rigid plane and loaded with two rigid blocks by using the finite element method (FEM).

A review of previous studies reveals that no prior work has analyzed the discontinuous contact problem for a system resting on a rigid plane, loaded by two different rigid blocks, and composed of both functionally graded and homogeneous layers. In this study, the DCCP of two layers with different material properties and resting on a rigid plane is solved analytically using elasticity theory and integral transformation techniques. When the studies so far are examined, it has been seen that generally, continuous contact problems, receding contact problems, friction contact problems are examined in functionally graded (FG) layers. It is determined that the layers in which the DCCPs are examined, in which the weight effect is taken into account, are mostly homogeneous layers. The studies investigating the solution for discontinuous contact conditions, in which the weight effects of both FG and homogeneous layer are considered and loaded with more than one block are very limited. Therefore, solution of this DCCP is conducted to contribute to the literature in this area.

2. Definition of the problem

The geometry of the DCCP is shown in Fig. 1. Layer (1) and layer (2) are assumed to be a functionally graded and a homogeneous layer, respectively. The density and shear modulus of the FG layer vary exponentially along the layer height, as given in Eqs. (a)-(b), while the shear modulus and density of the homogeneous layer are assumed to remain constant. In addition, the Poisson's ratios of the layers are assumed to be constant. The external loads P and Q are transmitted to the FG layer by two different rigid flat blocks. Body forces of the layers are included in the solution, and all contact surfaces are assumed frictionless.

$$\mu_1(y) = \mu_0 e^{\beta y}, \quad (-h_1 \leq y \leq 0) \tag{a}$$

$$\rho_1(y) = \rho_0 e^{\gamma y}, \quad (-h_1 \leq y \leq 0) \tag{b}$$

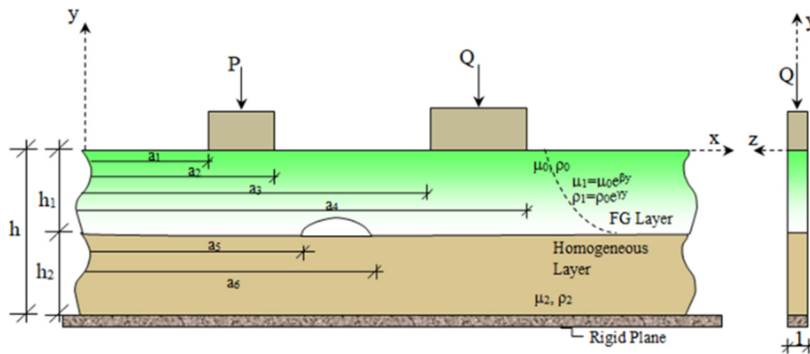


Figure 1. Geometry of DCCP

where μ_0 and ρ_0 denote the shear modulus and density at the top surface of the FG layer, respectively; β and γ are the stiffness and density parameters.

2.1 Analytical solution of discontinuous contact problem

$u(x,y)$ and $v(x,y)$ are displacement components, $\sigma_x(x,y)$, $\sigma_y(x,y)$ and $\tau_{xy}(x,y)$ are stress components and the boundary conditions of the problem can be written as follows according to the axis set in Fig. 1

$$\sigma_{y_1}(x, 0) = \begin{cases} -p_1(x) & a_1 < x < a_2 \\ -p_2(x) & a_3 < x < a_4 \\ 0 & -\infty < x < a_1, \quad a_2 < x < a_3, \quad a_4 < x < \infty \end{cases} \quad (1a)$$

$$\tau_{xy_1}(x, 0) = 0 \quad -\infty < x < \infty \quad (1b)$$

$$\tau_{xy_1}(x, -h_1) = 0 \quad -\infty < x < \infty \quad (1c)$$

$$\sigma_{y_1}(x, -h_1) = \sigma_{y_2}(x, -h_1) \quad -\infty < x < \infty \quad (1d)$$

$$\frac{\partial}{\partial x} [v_2(x, -h_1) - v_1(x, -h_1)] = \begin{cases} 0 & -\infty < x < a_5, a_6 < x < \infty \\ \Lambda(x) & a_5 < x < a_6 \end{cases} \quad (1e)$$

$$\tau_{xy_2}(x, -h_1) = 0 \quad -\infty < x < \infty \quad (1f)$$

$$\tau_{xy_2}(x, -h) = 0 \quad -\infty < x < \infty \quad (1g)$$

$$v_2(x, -h) = 0 \quad -\infty < x < \infty \quad (1h)$$

$p_1(x)$ and $p_2(x)$ in Eq. (1a) are the unknown contact stresses between the rigid block and the functionally graded (FG) layer.

The equilibrium conditions for the problem are

$$P = -\frac{1}{\mu_0} \int_{a_1}^{a_2} p_1(t) dt \quad (2a)$$

$$Q = -\frac{1}{\mu_0} \int_{a_3}^{a_4} p_2(t) dt \quad (2b)$$

When the boundary conditions given by Eqs. (1a)-(1h) are substituted into the stress and displacement expressions obtained previously in Kaya et al. [24], eight algebraic equations are obtained as follows

$$(\sigma_y)_1(x, 0) = \frac{\mu_0}{(K_1 - 1)} \sum_{j=1}^4 D_j M_j * = \int_{a_1}^{a_2} -p_1(t) e^{-i\zeta t} dt + \int_{a_3}^{a_4} -p_2(t) e^{-i\zeta t} dt \quad (3)$$

$$\sum_{j=1}^4 C_j M_j^* = 0 \quad (4)$$

$$\sum_{j=1}^4 C_j M_j^* e^{-s_j h_1} = 0 \quad (5)$$

$$\sum_{j=1}^4 E_j M_j^* e^{-h_1(s_j + \beta)} - \frac{\mu_2}{\mu_0} \left\{ e^{|\zeta| h_1} [-2|\zeta| N_1^* + ((K_2 - 1) + 2|\zeta| h_1) N_2^*] \right. \\ \left. + e^{-|\zeta| h_1} [2|\zeta| N_3^* + ((K_2 - 1) - 2|\zeta| h_1) N_4^*] \right\} = 0 \quad (6)$$

$$\sum_{j=1}^4 i\zeta n_j M_j^* e^{-s_j h_1} - i\zeta \{ (N_1^* - h_1 N_2^*) e^{|\zeta| h_1} + (N_3^* - h_1 N_4^*) e^{-|\zeta| h_1} \} = L \quad (7)$$

$$(\tau_{xy})_2(x, -h_1) = e^{|\zeta| h_1} \left\{ 2\zeta N_1^* - \left[\frac{|\zeta|}{\zeta} (K_2 + 1) + 2\zeta h_1 \right] N_2^* \right\} \\ + e^{-|\zeta| h_1} \left\{ 2\zeta N_3^* + \left[\frac{|\zeta|}{\zeta} (K_2 + 1) - 2\zeta h_1 \right] N_4^* \right\} = 0 \quad (8)$$

$$(\tau_{xy})_2(x, -h) = e^{|\zeta| h} \left\{ 2\zeta N_1^* - \left[\frac{|\zeta|}{\zeta} (K_2 + 1) 2\zeta h \right] N_2^* \right\} \\ + e^{-|\zeta| h} \left\{ 2\zeta N_3^* + \left[\frac{|\zeta|}{\zeta} (K_2 + 1) - 2\zeta h \right] N_4^* \right\} = 0 \quad (9)$$

$$[N_1^* - h N_2^*] e^{|\zeta| h} + [N_3^* - h N_4^*] e^{-|\zeta| h} = 0 \quad (10)$$

The expressions $\sigma_{y_1}(x, y)$, $\sigma_{y_2}(x, y)$, $\tau_{xy_1}(x, y)$, $\tau_{xy_2}(x, y)$ and L are given in Eqs. (11a)-(11f). In addition, other expressions are written in the supplementary section.

$$\sigma_{y_1}(x, y) = \frac{\mu_1(y)}{(\kappa_1 - 1)} \frac{1}{2\pi} \int_{-\infty}^{\infty} \sum_{j=1}^4 [i\xi(3 - \kappa_1) + s_j n_j (\kappa_1 + 1)] A_j e^{s_j y + i\xi x} d\xi \quad (11a)$$

$$\tau_{xy_1}(x, y) = \mu_1(y) \frac{1}{2\pi} \int_{-\infty}^{\infty} \sum_{j=1}^4 [s_j + i\xi n_j] A_j e^{s_j y + i\xi x} d\xi \quad (11b)$$

$$v_1(x, y) = \frac{1}{2\pi} \int_{-\infty}^{\infty} \sum_{j=1}^4 A_j n_j e^{s_j y + i\xi x} d\xi \quad (11c)$$

$$\sigma_{y_2}(x, y) = \frac{\mu_2}{2\pi} \int_{-\infty}^{+\infty} e^{i\xi x} \left\{ e^{-|\xi| y} \{ -2|\xi| B1 + [(\kappa_2 - 1) - 2|\xi| y] B2 \} \right. \\ \left. + e^{|\xi| y} \{ 2|\xi| B3 + [(\kappa_2 - 1) + 2|\xi| y] B4 \} \right\} d\xi \quad (11d)$$

$$\tau_{xy_2}(x, y) = \frac{i\mu_2}{2\pi} \int_{-\infty}^{+\infty} e^{i\xi x} \left\{ \begin{aligned} &e^{-|\xi|y} \left\{ 2\xi B1 + \left[-\frac{|\xi|}{\xi} (\kappa_2 + 1) - 2\xi y \right] B2 \right\} \\ &+ e^{|\xi|y} \left\{ 2\xi B3 + \left[\frac{|\xi|}{\xi} (\kappa_2 + 1) + 2\xi y \right] B4 \right\} \end{aligned} \right\} d\xi \quad (11e)$$

$$L = \frac{1}{2i\pi\zeta} \int_{a_5}^{a_6} \Lambda(t) dt \quad (11f)$$

K_1 and K_2 are material constants (Kolosov's constant) and are expressed as $K = (3 - \nu)/(1 + \nu)$ depending on the Poisson's ratio (ν). $M_1^*, \dots, M_4^*, N_1^*, \dots, N_4^*$ are obtained by replacing the boundary conditions in expressions (1a)-(1h) with stress and displacement expressions. Using (1i) and (1j), the singular integral equations can be obtained for $P(x)$ and $Q(x)$ after some simple operations as follow [27]

$$\begin{aligned} &-\frac{1}{\pi\mu_0} \int_{a_1}^{a_2} p_1(t_1) dt_1 \left[Y_1 \times (x_1, t_1) + \left(\frac{K_1 + 1}{4} \right) \frac{1}{(t_1 - x_1)} \right] \\ &-\frac{1}{\pi\mu_0} \int_{a_3}^{a_4} p_2(t_2) dt_2 \left[Y_1 \times (x_1, t_2) + \left(\frac{K_1 + 1}{4} \right) \frac{1}{(t_2 - x_1)} \right] = 0 \quad a_1 < x < a_2 \end{aligned} \quad (12a)$$

$$\begin{aligned} &-\frac{1}{\pi\mu_0} \int_{a_1}^{a_2} p_1(t_1) dt_1 \left[Y_1 * (x_2, t_1) + \left(\frac{K_1 + 1}{4} \right) \frac{1}{(t_1 - x_2)} \right] \\ &-\frac{1}{\pi\mu_0} \int_{a_3}^{a_4} p_2(t_2) dt_2 \left[Y_1 * (x_2, t_2) + \left(\frac{K_1 + 1}{4} \right) \frac{1}{(t_2 - x_2)} \right] = 0 \quad a_3 < x < a_4 \end{aligned} \quad (12b)$$

The Y_1 kernel in equations is defined as follows

$$Y_1(x, t) = \zeta(M_1 n_1 + M_2 n_2 + M_3 n_3 + M_4 n_4) \quad (13)$$

$$Y_1 \times (x, t) = \int_0^\infty \left(Y_1(x, t) - \left(\frac{K_1 + 1}{4} \right) \sin \zeta(t - x) \right) d\zeta \quad (14)$$

Where $Y_1(x, t)$ is Fredholm's kernel of singular integral equations. The stress relationship between the layers is defined as

$$\left[(\sigma_y)_1(x, -h_1) \right] + \frac{\rho_0 g (e^{-\gamma h_1} - 1)}{\gamma} = 0 \quad a_5 < x < a_6 \quad (15)$$

$$\begin{aligned} \frac{\partial v_1(x, y)}{\partial x} = &-\frac{1}{2\mu_0\pi} \int_{a_1}^{a_2} p_1(t) e^{-i\zeta t} dt \int_{-\infty}^{\infty} i e^{i\zeta x} \left(\zeta M_1 n_1 e^{s_1 y} + \zeta M_2 n_2 e^{s_2 y} \right. \\ &\left. + \zeta M_3 n_3 e^{s_3 y} + \zeta M_4 n_4 e^{s_4 y} \right) d\zeta \\ &-\frac{1}{2\mu_0\pi} \int_{a_3}^{a_4} p_2(t) e^{-i\zeta t} dt \int_{-\infty}^{\infty} i e^{i\zeta x} \left(\zeta M_1 n_1 e^{s_1 y} + \zeta M_2 n_2 e^{s_2 y} \right. \\ &\left. + \zeta M_3 n_3 e^{s_3 y} + \zeta M_4 n_4 e^{s_4 y} \right) d\zeta \\ &+\frac{1}{2i\pi} \int_{a_5}^{a_6} \Lambda(t) e^{-i\zeta t} dt \int_{-\infty}^{\infty} i e^{i\zeta x} \left(\zeta M_1 ** n_1 e^{s_1 y} + \zeta M_2 ** n_2 e^{s_2 y} \right. \\ &\left. + \zeta M_3 ** n_3 e^{s_3 y} + \zeta M_4 ** n_4 e^{s_4 y} \right) d\zeta \end{aligned} \quad (16)$$

In this case, the integral equations obtained from Eqs. (1i) and (1j) at the intervals $a_1 < x < a_2$ and $a_3 < x < a_4$ can be arranged as follows

$$\begin{aligned} & -\frac{1}{\pi\mu_0} \int_{a_1}^{a_2} p_1(t_1) dt_1 \left[Y_1 * (x_1, t_1) + \left(\frac{K_1 + 1}{4} \right) \frac{1}{(t_1 - x_1)} \right] \\ & -\frac{1}{\pi\mu_0} \int_{a_3}^{a_4} p_2(t_2) dt_2 \left[Y_1 * (x_1, t_2) + \left(\frac{K_1 + 1}{4} \right) \frac{1}{(t_2 - x_1)} \right] \\ & + \frac{1}{\pi} \int_{a_5}^{a_6} \Lambda(t_3) dt_1 [Y_{22}(x_1, t_3)] = 0 \end{aligned} \quad a_1 < x < a_2 \quad (17)$$

$$\begin{aligned} & -\frac{1}{\pi\mu_0} \int_{a_1}^{a_2} p_1(t_1) dt_1 \left[Y_1 * (x_1, t_1) + \left(\frac{K_1 + 1}{4} \right) \frac{1}{(t_1 - x_2)} \right] \\ & -\frac{1}{\pi\mu_0} \int_{a_3}^{a_4} p_2(t_2) dt_2 \left[Y_1 * (x_1, t_2) + \left(\frac{K_1 + 1}{4} \right) \frac{1}{(t_2 - x_2)} \right] \\ & + \frac{1}{\pi} \int_{a_5}^{a_6} \Lambda(t_3) dt_1 [Y_{22}(x_2, t_3)] = 0 \end{aligned} \quad a_3 < x < a_4 \quad (18)$$

Its expression in the integral equation is defined by equation kernels are given below

$$Y_1(x, t) = \int_0^\infty \zeta (M_1 n_1 + M_2 n_2 + M_3 n_3 + M_4 n_4) [\cos \zeta (t - x)] d\zeta \quad (19)$$

$$Y_{22}(x, t) = \int_0^\infty \zeta (M_1 ** n_1 + M_2 ** n_2 + M_3 ** n_3 + M_4 ** n_4) [\cos \zeta (t - x)] d\zeta \quad (20)$$

The third equation used to determine the unknown functions is Eq. (15).

For the case where the mass forces are taken into account, the coefficients are written in their place in the vertical stress expression and if necessary actions are taken

$$\begin{aligned} (\sigma_y)_1(x, y) = & \frac{\mu_0 e^{\beta y}}{(K_1 - 1)} \left\{ -\frac{1}{\pi\mu_0} \int_{a_1}^{a_2} p_1(t) dt \int_0^\infty \sum D_j M_j e^{s_j y} \cos \zeta (t - x) d\zeta \right. \\ & -\frac{1}{\pi\mu_0} \int_{a_3}^{a_4} p_2(t) dt \int_0^\infty \sum D_j M_j e^{s_j y} \cos \zeta (t - x) d\zeta \\ & \left. -\frac{1}{\pi} \int_{a_5}^{a_6} \Lambda(t) dt \int_0^\infty \sum D_j M_j ** e^{s_j y} i \sin \zeta (t - x) d\zeta \right\} + \frac{\rho_0 g (e^{\gamma y} - 1)}{\gamma} = 0 \end{aligned} \quad (21)$$

In the above equation, when passing to the $y \rightarrow -h_1$ limit, when the numerator is divided by the denominator, singular terms that break the complaint of the integral equation arise. The singular terms determined as

$$ST_2 = \int_0^\infty e^{-\zeta(h_1 + y)} \left[-\frac{4 \left(\frac{\mu_2}{\mu_0} \right)}{(1 + K_2) + e^{\beta h_1} \left(\frac{\mu_2}{\mu_0} \right) (1 + K_1)} \right] \sin \zeta (t - x) d\zeta dt \quad (22)$$

This term, which distorts the convergence, has been removed from the integral Eq. (21), after the

closed integral of the equation numbered (22) with the help of integral transform tables, the limit of $y \rightarrow -h_1$ is passed. When these operations are done, the third integral equation can be expressed as follows.

$$\begin{aligned} & -\frac{1}{\pi} \int_{a_1}^{a_2} p_1(t) dt [Y_2(x, t) \cos \zeta (t - x)] - \frac{1}{\pi} \int_{a_3}^{a_4} p_2(t) dt [Y_2(x, t) \cos \zeta (t - x)] \\ & - \frac{\mu_0}{\pi} \int_{a_5}^{a_6} \Lambda(t) dt [Y_4 * (x, t) i \sin \zeta (t - x)] d\zeta - \frac{4 \left(\frac{\mu_2}{\mu_0} \right)}{(1 + K_2) + e^{\beta h_1} \left(\frac{\mu_2}{\mu_0} \right) (1 + K_1)} \frac{1}{(t - x)} \quad (23) \\ & = - \frac{(e^{\gamma h_1} - 1)}{\gamma h_1} \frac{1}{\lambda_1} \quad a_5 < x < a_6 \end{aligned}$$

The $Y_4(x, t)$ and $Y_4^*(x, t)$ equations are

$$Y_4(x, t) = \int_0^\infty \left(\frac{e^{\beta y}}{(K_1 - 1)} \sum_{j=1}^4 F_j M_j * e^{s_j y} \sin \zeta (t - x) \right) d\zeta \quad (24)$$

$$Y_4 * (x, t) = \int_0^\infty \left(Y_4(x, t) - \left[- \frac{4 \left(\frac{\mu_2}{\mu_0} \right)}{(1 + K_2) + e^{\beta h_1} \left(\frac{\mu_2}{\mu_0} \right) (1 + K_1)} \right] \sin \zeta (t - x) \right) d\zeta \quad (25)$$

$$x_1 = \frac{a_2 - a_1}{2} r_1 + \frac{a_2 + a_1}{2}, \quad t_1 = \frac{a_2 - a_1}{2} s_1 + \frac{a_2 + a_1}{2} \quad (26a,b)$$

$$x_2 = \frac{a_4 - a_3}{2} r_2 + \frac{a_4 + a_3}{2}, \quad t_2 = \frac{a_4 - a_3}{2} s_2 + \frac{a_4 + a_3}{2} \quad (26c,d)$$

$$\alpha_1(s_1) = \frac{p_1 \left(\frac{a_2 - a_1}{2} s_1 + \frac{a_2 + a_1}{2} \right)}{\frac{P}{h_1}}, \quad \alpha_2(s_2) = \frac{p_2 \left(\frac{a_4 - a_3}{2} s_2 + \frac{a_4 + a_3}{2} \right)}{\frac{P}{h_1}} \quad (26e,f)$$

$$x_3 = \frac{a_6 - a_5}{2} r_3 + \frac{a_6 + a_5}{2}, \quad t_3 = \frac{a_6 - a_5}{2} s_3 + \frac{a_6 + a_5}{2} \quad (26g,h)$$

$$\alpha_3(s_3) = \frac{\mu_1 \Lambda \left(\frac{a_6 - a_5}{2} s_3 + \frac{a_6 + a_5}{2} \right)}{\frac{P}{h_1}} \quad (26i)$$

If the expressions (26a)-(26i) are written in Eqs. (17), (18) and (23), then the equations are obtained as

$$- \sum_{i=1}^n W_i G_1(s_{1i}) \frac{a_2 - a_1}{2h_1} \left[\eta_1 * (r_{1j}, s_{1i}) + \left(\frac{K_1 + 1}{4} \right) \frac{1}{\frac{a_2 - a_1}{2} (s_{1i} - r_{1j})} \right] \quad (27)$$

$$\begin{aligned}
& - \sum_{i=1}^n W_i G_2(s_{2i}) \frac{a_4 - a_3}{2h_1} \left[\eta_2 * (r_{1j}, s_{2i}) + \left(\frac{K_1 + 1}{4} \right) \frac{1}{\left[\frac{a_4 - a_3}{2} s_{2i} + \frac{a_4 + a_3}{2} \right] - \left[\frac{a_2 - a_1}{2} r_{1j} + \frac{a_2 + a_1}{2} \right]} \right] \\
& - \sum_{i=1}^n W_i G_3(s_{3i}) \frac{a_6 - a_5}{2h_1} \eta_3 * (r_{1j}, s_{3i}) = 0 \quad (j = 1, \dots, n-1)
\end{aligned} \quad (27)$$

$$\begin{aligned}
& - \sum_{i=1}^n W_i G_1(s_{1i}) \frac{a_2 - a_1}{2h_1} \left[\eta_4 * (r_{2j}, s_{1i}) + \left(\frac{K_1 + 1}{4} \right) \frac{1}{\left[\frac{a_2 - a_1}{2} s_{1i} + \frac{a_2 + a_1}{2} \right] - \left[\frac{a_4 - a_3}{2} r_{2j} + \frac{a_4 + a_3}{2} \right]} \right] \\
& - \sum_{i=1}^n W_i G_2(s_{2i}) \frac{a_4 - a_3}{2h_1} \left[\eta_5 * (r_{2j}, s_{2i}) + \left(\frac{K_1 + 1}{4} \right) \frac{1}{\frac{a_4 - a_3}{2} (s_{2j} - r_{2i})} \right] \\
& - \sum_{i=1}^n W_i G_3(s_{3i}) \frac{a_6 - a_5}{2h_1} \eta_6 * (r_{2j}, s_{3i}) = 0 \quad (j = 1, \dots, n-1)
\end{aligned} \quad (28)$$

$$\begin{aligned}
& - \sum_{i=1}^n W_i G_1(s_{1i}) \frac{a_2 - a_1}{2h_1} \eta_7 * (r_{3j}, s_{1i}) ds_3 - \sum_{i=1}^n W_i G_2(s_{2i}) \frac{a_4 - a_3}{2h_1} \eta_8 * (r_{3j}, s_{2i}) ds_3 \\
& - \sum_{i=1}^n W_i G_3(s_{3i}) \frac{a_6 - a_5}{2h_1} \left[\eta_9 * (r_{3j}, s_{3i}) - \frac{4 \left(\frac{\mu_2}{\mu_0} \right)}{(1 + K_2) + e^{\beta h_1} \left(\frac{\mu_2}{\mu_0} \right) (1 + K_1)} \frac{1}{\frac{a_6 - a_5}{2h_1} (s_{3i} - r_{3j})} \right] \\
& = - \frac{(e^{-\gamma h} - 1)}{\gamma h_1} \frac{1}{\lambda_1} \quad (j = 1, \dots, n-1)
\end{aligned} \quad (29)$$

$$\begin{aligned}
\eta_1 * (r_1, s_1) &= Y_1 * (x_1, t_1), & \eta_2 * (r_1, s_2) &= Y_1 * (x_1, t_2), & \eta_1 * (r_1, s_3) &= Y_{22}(x_1, t_3), \\
\eta_4 * (r_2, s_1) &= Y_1 * (x_2, t_1), & \eta_5 * (r_2, s_2) &= Y_1 * (x_2, t_2), & \eta_6 * (r_2, s_3) &= Y_{22}(x_2, t_3), \\
\eta_7 * (r_3, s_1) &= Y_2(x_3, t_1), & \eta_8 * (r_3, s_2) &= Y_2(x_3, t_2), & \eta_9 * (r_3, s_3) &= Y_4 * (x_3, t_3)
\end{aligned} \quad (30)$$

equations are obtained. Where, $\alpha_1(s_1)$, $\alpha_2(s_2)$ are the dimensionless contact stress occurred under the rigid blocks and $\alpha_3(s_3)$ is the slope function. Since $\alpha(s)$ has singularity in $\pm s_1$, the index of integral equation +1, and the solution can be taken as follows

$$\alpha_i(s_i) = G_i(s_i) [1 - s_i^2]^{-\frac{1}{2}} \quad (-1 < s_i < 1) \quad (i = 1, 2, 3) \quad (31)$$

If the optimal Gauss-Chebyshev integration formula is applied to Eqs. (27)-(29)

$$\begin{aligned}
& - \sum_{i=1}^n W_i G_1(s_{1i}) \frac{a_2 - a_1}{2h_1} \left[\eta_1 * (r_{1j}, s_{1i}) + \left(\frac{K_1 + 1}{4} \right) \frac{1}{\frac{a_2 - a_1}{2} (s_{1i} - r_{1j})} \right] \\
& - \sum_{i=1}^n W_i G_2(s_{2i}) \frac{a_4 - a_3}{2h_1} \left[\eta_2 * (r_{1j}, s_{2i}) + \left(\frac{K_1 + 1}{4} \right) \frac{1}{\left[\frac{a_4 - a_3}{2} s_{2i} + \frac{a_4 + a_3}{2} \right] - \left[\frac{a_2 - a_1}{2} r_{1j} + \frac{a_2 + a_1}{2} \right]} \right] \\
& - \sum_{i=1}^n W_i G_3(s_{3i}) \frac{a_6 - a_5}{2h_1} \eta_3 * (r_{1j}, s_{3i}) = 0 \quad (j = 1, \dots, n-1)
\end{aligned} \quad (32)$$

$$\begin{aligned}
& - \sum_{i=1}^n W_i G_1(s_{1i}) \frac{a_2 - a_1}{2h_1} \left[\eta_4 * (r_{2j}, s_{1i}) + \left(\frac{K_1 + 1}{4} \right) \frac{1}{\left[\frac{a_2 - a_1}{2} s_{1i} + \frac{a_2 + a_1}{2} \right] - \left[\frac{a_4 - a_3}{2} r_{2j} + \frac{a_4 + a_3}{2} \right]} \right] \\
& - \sum_{i=1}^n W_i G_2(s_{2i}) \frac{a_4 - a_3}{2h_1} \left[\eta_5 * (r_{2j}, s_{2i}) + \left(\frac{K_1 + 1}{4} \right) \frac{1}{\frac{a_4 - a_3}{2} (s_{2j} - r_{2i})} \right] \\
& - \sum_{i=1}^n W_i G_3(s_{3i}) \frac{a_6 - a_5}{2h_1} \eta_6 * (r_{2j}, s_{3i}) = 0 \quad (j = 1, \dots, n-1)
\end{aligned} \tag{33}$$

$$\begin{aligned}
& - \sum_{i=1}^n W_i G_1(s_{1i}) \frac{a_2 - a_1}{2h_1} \eta_7 * (r_{3j}, s_{1i}) ds_3 - \sum_{i=1}^n W_i G_2(s_{2i}) \frac{a_4 - a_3}{2h_1} \eta_8 * (r_{3j}, s_{2i}) ds_3 \\
& - \sum_{i=1}^n W_i G_3(s_{3i}) \frac{a_6 - a_5}{2h_1} \left[\eta_9 * (r_{3j}, s_{3i}) - \frac{4 \left(\frac{\mu_2}{\mu_0} \right)}{(1 + K_2) + e^{\beta h_1} \left(\frac{\mu_2}{\mu_0} \right) (1 + K_1)} \frac{1}{\frac{a_6 - a_5}{2h_1} (s_{3i} - r_{3j})} \right] \\
& = - \frac{(e^{-\gamma h} - 1)}{\gamma h_1} \frac{1}{\lambda_1} \quad (j = 1, \dots, n-1)
\end{aligned} \tag{34}$$

Using the optimal Gauss-Chebyshev integration formulas, the dimensionless quantities and single-valued conditions of the problem are given below

$$\sum_{i=1}^n \pi W_i \frac{a_2 - a_1}{2h_1} G_1(s_{1i}) = 1 \tag{35a}$$

$$\sum_{i=1}^n \pi W_i \frac{a_4 - a_3}{2h_1} G_2(s_{2i}) = \frac{Q}{P} \tag{35b}$$

$$\sum_{i=2}^{n-1} \pi W_i \frac{a_6 - a_5}{2h_1} G_3(s_{3i}) = 0 \tag{35c}$$

equations are obtained.

The terms in these equations are defined as follows

$$W_1 = W_n = \frac{1}{2n-2}, \quad W_i = \frac{1}{n-1} \quad (i = 1, \dots, n-1) \tag{36}$$

$$s_{1i} = s_{2i} = \cos \left(\frac{i-1}{n-1} \pi \right) \quad (i = 1, \dots, n-1) \tag{37}$$

$$s_{3i} = \cos \left(\frac{i-1}{n-1} \pi \right) \quad (i = 1, \dots, n-1) \tag{38}$$

$$r_{1i} = r_{2i} = r_{3i} = \cos \left(\frac{2j-1}{2n-2} \pi \right) \quad (j = 1, \dots, n-1) \tag{39}$$

In order to determine the displacement difference $[v_2(x, -h_1) - v_1(x, -h_1)]$ in the separation zone between (e, f), in other words, the separation that occurs at the interface of the FG layer and the homogeneous layer

$$v \times (x, -h_1) = v_2(x, -h_1) - v_1(x, -h_1) = \int_{a_5}^x \alpha_3(t) dt \quad (a_5 < x < a_6) \quad (40)$$

$$\frac{\mu_0}{P} v \times (x, -h_1) = \frac{a_6 - a_5}{2h_1} \int_{-1}^{r_3} \alpha_3(t) dt \quad (-1 < r_3 < 1) \quad (41)$$

$$x = \frac{a_6 - a_5}{2} r_3 + \frac{a_6 + a_5}{2} \quad (42)$$

If it is written as above and the index of Eq. (41) is taken as +1, solution of the equation

$$\frac{\mu_0}{P} v \times (x, -h_1) = \frac{a_6 - a_5}{2h_1} \sum_{i=2}^{m-1} W_i G_3(s_{3i}) \quad (m = 2, \dots, n-1) \quad (43)$$

It can be searched as above, and the separations occurring between layers can be determined. In addition, the critical load factors (λ_{cr}) are presented as

$$\lambda_{cr1} = \frac{P_{cr1}}{\rho_0 g h_1^2} \quad (44)$$

$$\lambda_{cr2} = \frac{P_{cr2}}{\rho_0 g h_1^2} \quad (45)$$

3. Results and discussions

In Fig. 2, the plot of the dimensionless $\sigma_{1y}(x, -h_1)/P/h_1$ stress distribution according to the stiffness parameter change is given. As the stiffness parameter increases (i.e., as the layer becomes less stiff along its depth), the separation zone increases. Also, as βh_1 values increased, the point where separation started moved away from the second block. In addition, when Table 1 is examined, separation starting and ending points are seen according to the change of the critical load factor with the stiffness parameter. As it can be understood from the table, when the stiffness parameter is taken constant and the load factor is decreased, a smaller separation zone is formed. In addition, as the load decreased, the starting point of separation moved away from the second block. It can be seen from the table that the separation zone grows when the load factor is taken constant and the stiffness parameter is reduced towards the bottom of the layer.

In Fig. 3, the plot of the dimensionless stress distribution $\sigma_{1y}(x, -h_1)/P/h_1$ according to density parameter change (γh_1) is given. When Fig. 3 is examined, the separation distances increased as γh_1 values increased, that is, as the density decreased along the depth of the layer.

In Fig. 4, the stress distribution at the interface of the layers according to the change in distance between blocks ($(a_3 - a_2)/h_1$) is given. Stress values decreased as the blocks moved away from each

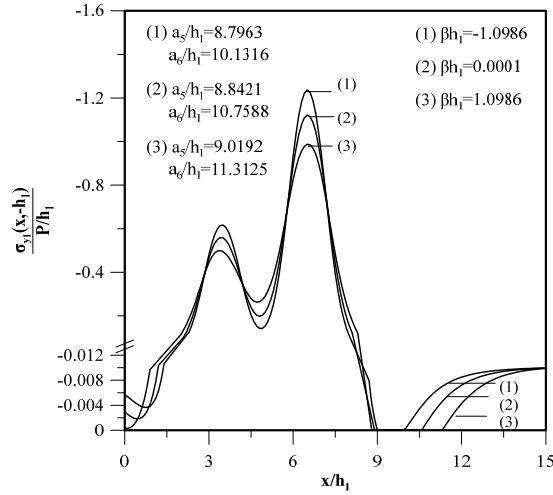


Figure 2. Dimensionless stress distribution $\sigma_{1y}(x, -h_1)/P/h_1$ between layers according to stiffness parameter (βh_1) change ($a_1/h_1 = 3$; $(a_2 - a_1)/h_1 = 1$; $(a_3 - a_2)/h_1 = 2$; $(a_4 - a_3)/h_1 = 1$; $\mu_0 = 1$; $Q = 2P$; $\gamma h_1 = -1.0986$; $K_1 = 2$; $K_2 = 2$; $y = -h_1$; $h_1/h_2 = 0.5$; $\mu_2/\mu_{-h_1} = 1$; $\lambda = 180 > \lambda_{cr1}$)

Table 1. Separation starting and ending points between layers according to stiffness parameter (βh_1) and load factor (λ) variation ($a_1/h_1 = 3$; $(a_2 - a_1)/h_1 = 1$; $(a_3 - a_2)/h_1 = 2$; $(a_4 - a_3)/h_1 = 1$; $\mu_0 = 1$; $Q = 2P$; $\gamma h_1 = -1.0986$; $K_1 = 2$; $K_2 = 2$; $y = -h_1$; $h_1/h_2 = 0.5$; $\mu_2/\mu_{-h_1} = 1$)

λ	$\beta h_1 = -0.4055$		$\beta h_1 = 0.0001$		$\beta h_1 = 0.4055$	
	a_5/h_1	a_6/h_1	a_5/h_1	a_6/h_1	a_5/h_1	a_6/h_1
80	9.2761	9.7023	9.2913	9.9304	9.3196	10.0516
85	9.2203	9.7416	9.2507	9.9852	9.2931	10.1463
90	9.1622	9.7823	9.1802	10.0666	9.2354	10.3266
95	9.1140	9.8135	9.1348	10.1173	9.1807	10.4397

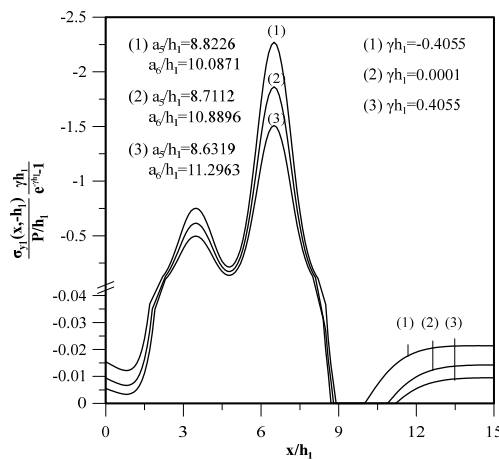


Figure 3. Dimensionless stress distribution $\sigma_{1y}(x, -h_1)/P/h_1$ between layers according to density parameter (γh_1) change ($a_1/h_1 = 3$; $(a_2 - a_1)/h_1 = 1$; $(a_3 - a_2)/h_1 = 2$; $(a_4 - a_3)/h_1 = 1$; $\mu_0 = 1$; $Q/P = 2$; $\beta h_1 = -1.0986$; $K_1 = 2$; $K_2 = 2$; $y = -h_1$; $h_1/h_2 = 2$; $\mu_2/\mu_{-h_1} = 1$; $\lambda = 180 > \lambda_{cr1}$)

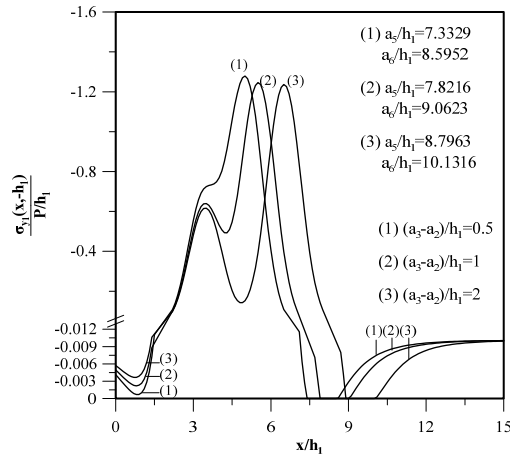


Figure 4. Dimensionless stress distribution $\sigma_{1y}(x, -h_1)/P/h_1$ between layers according to the change of distance between blocks ($(a_3 - a_2)/h_1$) ($a_1/h_1 = 3$; $(a_2 - a_1)/h_1 = 1$; $(a_4 - a_3)/h_1 = 1$; $Q/P = 2$; $\beta h_1 = -1.0986$; $\gamma h_1 = -1.0986$; $K_1 = 2$; $K_2 = 2$; $y = -h_1$; $h_2/h_1 = 2$; $\mu_2/\mu_{-h_1} = 1$; $\lambda = 180 > \lambda_{cr1}$)

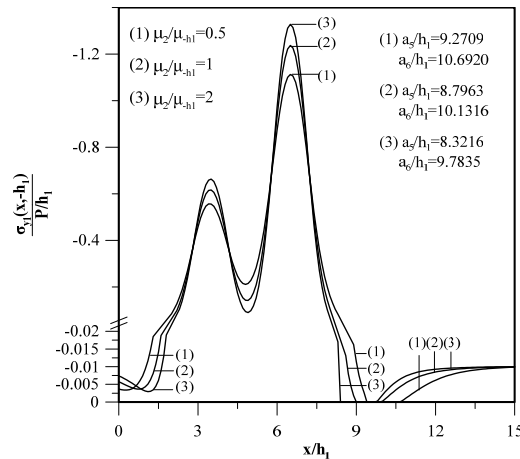


Figure 5. Dimensionless stress distribution $\sigma_{1y}(x, -h_1)/P/h_1$ between layers according to the change of shear modulus ratio (μ_2/μ_{-h_1}) of the layers ($a_1/h_1 = 3$; $(a_2 - a_1)/h_1 = 1$; $(a_3 - a_2)/h_1 = 2$; $(a_4 - a_3)/h_1 = 1$; $Q/P = 2$; $\beta h_1 = -1.0986$; $\gamma h_1 = -1.0986$; $K_1 = 2$; $K_2 = 2$; $y = -h_1$; $h_2/h_1 = 2$; $\lambda = 180 > \lambda_{cr1}$)

other. There was also an increase in the departure starting and ending distances. As the distance between blocks decreased, the blocks interacted with each other more, there was an increase in stress values. With this graph, it can be understood how important the interaction between blocks is not only in continuous contact but also in discontinuous contact.

The dimensionless $\sigma_{1y}(x, -h_1)/P/h_1$ stress distribution according to the ratio of the shear modulus of the homogeneous layer and the shear modulus of the lower surface of the functionally graded layer (μ_2/μ_{-h_1}) is given in Fig. 5. When the shear modulus of the homogeneous plane decreases compared to the shear modulus of the bottom surface of the FG layer, a decrease in the stress values has been observed. In addition, it has been observed that the starting point of separation moves away

as the ratio decreases. While performing all these analyses, only the loads that would cause separation in a region between the FG layer and the homogeneous layer were selected ($\lambda_{cr2} > \lambda > \lambda_{cr1}$). Attention has been paid to the fact that the selected loads are at the bottom of the block, to the left of the FG layer and that will not create separation between the homogeneous layer and the rigid plane.

In addition, if the height of the homogeneous layer is increased, the problem is similar to Polat [28]. Table 2 shows that the height of the homogeneous layer is increased and the separation starting and ending points were determined according to the stiffness parameter change and compared with Polat [28]. When the table is examined, it is seen that as the stiffness parameter increases, the starting and ending points of the separation move away from the second block and the results are quite compatible with the study in the literature.

Similar to the study conducted by Polat [28], Bora [29] reported that when the stiffness of the elastic half-plane is significantly increased, the medium behaves as a rigid plane. Likewise, in the present study, when the stiffness parameter (βh_1) and density parameter (γh_1) of the upper FG layer is taken as 0.0001, the layer exhibits the behavior of a homogeneous layer. Therefore, the two studies are comparable in terms of boundary conditions of the system. In his study, Bora [29] performed additional analyses by varying the stiffness of the elastic half-plane for different parameters. The results obtained in the present work were compared with those of Bora's study, and it was observed that the analyses performed for $\beta h_1 = \gamma h_1 = 0.0001$ showed similar tendencies. The comparison results are presented in Tables 3 and 4.

If the applied load is greater than the initial separation load ($\lambda > \lambda_{cr1}$), the vertical displacement difference [$v_1(x, -h_1) - v_2(x, -h_1)$], that is, the separations between the FG layer and the homogeneous layer, Stiffness parameter variation (βh_1), density parameter variation (γh_1), change in distance between blocks $(a_3 - a_2)/h_1$ and variation of layers with shear modulus ratio (μ_2/μ_{-h_1}) are discussed

Table 2. Separation starting and ending points between layers according to stiffness parameter (βh_1) and compared with [28] ($a_1/h_1 = 3$; $(a_2 - a_1)/h_1 = 1$; $(a_3 - a_2)/h_1 = 2$; $(a_4 - a_3)/h_1 = 1$; $\mu_0 = 1$; $Q = 2P$; $\gamma h_1 = 0.4055$; $K_1 = 2$; $K_2 = 2$; $y = -h_1$; $h_1/h = 0.1$; $\mu_2/\mu_{-h_1} = 1$; $\lambda = 105 > \lambda_{cr1}$)

βh_1	a_5/h_1		Error (%)	a_6/h_1		Error (%)
	This study	Polat (2019)		This study	Polat (2019)	
-0.4055	8.7331	8.7472	0.161	10.9013	10.8996	0.016
0.0001	8.8023	8.8065	0.048	11.2564	11.2348	0.192
0.4055	8.8798	8.8873	0.084	11.6708	11.5634	0.928

Table 3. Separation starting and ending points between layers according to stiffness parameter (βh_1) and compared with [28] ($a_1/h_1 = 3$; $(a_2 - a_1)/h_1 = 1$; $(a_3 - a_2)/h_1 = 2$; $(a_4 - a_3)/h_1 = 1$; $\mu_0 = 1$; $Q = 2P$; $\gamma h_1 = 0.4055$; $K_1 = 2$; $K_2 = 2$; $y = -h_1$; $h_1/h = 0.1$; $\mu_2/\mu_{-h_1} = 1$; $\lambda = 105 > \lambda_{cr1}$)

βh_1	a_5/h_1		Error (%)	a_6/h_1		Error (%)
	This study	Polat (2019)		This study	Polat (2019)	
-0.4055	8.7331	8.7472	0.161	10.9013	10.8996	0.016
0.0001	8.8023	8.8065	0.048	11.2564	11.2348	0.192
0.4055	8.8798	8.8873	0.084	11.6708	11.5634	0.928

according to various dimensionless sizes. Fig. 6 shows the separation graph between the layers according to the stiffness parameter change (βh_1). If the stiffness decreased towards the bottom of the FG layer, the difference in displacements was greater in addition to the increase in the separation zones. While the starting points of the separation were very close to each other, the end points moved away from the second block as the rigidity parameter increased. Fig. 7 shows the separation graph between the layers according to the density parameter change (γh_1). As can be seen from the graph, as the layer density FG decreased towards the lower part of the layer, that is, as the (γh_1) value increased, an increase in the swelling occurred.

According to the change in distance between blocks ($(a_3 - a_2)/h_1$), the separation graph between the layers interface is given in Fig. 8. As the blocks moved away from each other, shrinkage was observed in the separation zones. Fig. 9 shows the plot of the separations ($\mu_2/\mu_{.h1}$) of the shear modulus ratio of the homogeneous layer according to the shear modulus ratio of the lower surface of the FG layer. As the stiffness of the lower layer decreases according to the stiffness of the lower surface of the upper layer, i.e., ($\mu_2/\mu_{.h1}$) ratio decreases, the separation zone becomes smaller and the amount of swelling decreases.

4. Conclusions

The DCCP of two layers, one FG layer and the other homogeneous layer, loaded with two different rigid blocks and resting on a rigid plane, is solved analytically. Linear elasticity theory is used for the analytical solution. The separation conditions that occur at the layer interfaces when the load factor is greater than the critical load ($\lambda > \lambda_{cr}$) is investigated. Considering the weights of the layers, it was observed that the separated layer came into contact with the interfaces again, forming a limited separation zone. After the critical loads of the contact surfaces are determined, the loads that will not create discontinuities on the two contact surfaces at the same time are selected and discontinuities are determined for various dimensionless quantities. Continuous contact and discontinuous contact areas are seen in problem solving. $\sigma_{y1}(x, -h_1)/P/h_1$ increases from the edge of the first block and takes its maximum value under the block. As it approaches between the blocks, the stress values decrease, then increase again and reach its maximum value under the second block. Then, the stress value decreases again and becomes zero at the point where the separation between the layers begins and remains zero throughout the separation region ($a_5/h_1, a_6/h_1$).

- After the separation ending point, the stress values increase and converge to the critical load factor λ_{cr} . The starting point of the separation decrease as the stiffness parameter (βh_1) decreases for the same loading condition; consequently, the starting point of the separation moves away from the second block. However, when the stiffness parameter increases, in other words, in case of the stiffness of the FG layer decreases from top to bottom, the ending point of the separation moves away from the second block.
- Like the stiffness parameter, the starting point of the separation increases and the end point of the separation increases with a decreasing density parameter (γh_1).
- As the distance between blocks ($(a_3 - a_2)/h_1$) decreased, the blocks interacted with each other more, there is an increase in stress values. There is also an increase in the separation starting and ending distances.
- When the shear modulus of the homogeneous plane decreases compared to the shear modulus of the lower surface of the functionally graded layer, a decrease in the stress values is observed. Moreover, it was determined that as the ratio decreases, the starting point of separation moves

away from the second block.

References

1. Hussain, M., Naeem, M.N., Tounsi, A. (2020). Numerical study for nonlocal vibration of orthotropic SWCNTs based on Kelvin's model. *Advances in Concrete Construction*, 9(3), 301-312. <https://doi.org/10.12989/acc.2020.9.3.301>.
2. Singh, N.S., Thokchom, S., Debbarma, R. (2021). Correlation study on microstructure and mechanical properties of rice husk ash-Sodium aluminate geopolymer pastes. *Advances in Concrete Construction*, 11(1), 73-80. <https://doi.org/10.12989/acc.2021.11.1.073>.
3. Hussain, M., Asghar, S., Khadimallah, M.A., Ayed, H., Banoqitah, E.M., Loukil, H., Ali, I., Mahmoud, S.R., Tounsi, A. (2022). Elastic shell model: Effect of Young's Modulus on the vibration of double-walled CNTs. *Advances in Concrete Construction*, 13(6), 471-479. <https://doi.org/10.12989/acc.2022.13.6.471>.
4. Khan, M.A., Ahmad, S., Al-Osta, M., Al-Gahtani, H. (2023). Effect of fiber content on the performance of UHPC slabs under impact loading-experimental and analytical investigation. *Advances in Concrete Construction, An International Journal*, 15(3), 161-170. <https://doi.org/10.12989/acc.2023.15.3.161>
5. Chen, W.T., Engel, P.A. (1972). Impact and contact stress analysis in multilayer media. *International Journal of Solids and Structures*, 8(11), 1257-1281. [https://doi.org/10.1016/0020-7683\(72\)90079-0](https://doi.org/10.1016/0020-7683(72)90079-0).
6. Keer, L.M., Miller, G.R. (1983). Contact between an elastically supported circular plate and a rigid indenter. *International Journal of Engineering Science*, 21, 681-690. [https://doi.org/10.1016/0020-7225\(83\)90113-1](https://doi.org/10.1016/0020-7225(83)90113-1).
7. Geçit, M.R. (1986). Axisymmetric contact problem for a semiinfinite cylinder and a half space. *International Journal of Engineering Science*, 24(8), 1245-1256. [https://doi.org/10.1016/0020-7225\(86\)90054-6](https://doi.org/10.1016/0020-7225(86)90054-6).
8. Çakıroğlu, F.L., Çakıroğlu, M., Erdöl, R. (2001). Contact problems for two elastic layers resting on elastic half-plane. *Journal of Engineering Mechanics*, 127(2), 113-118. [https://doi.org/10.1061/\(ASCE\)0733-9399\(2001\)127:2\(113\)](https://doi.org/10.1061/(ASCE)0733-9399(2001)127:2(113)).
9. Yaylacı, M., Avcar, M. (2020). Finite Element Modeling of Contact Between an Elastic Layer and Two Elastic Quarter Planes. *Computers and Concrete, An International Journal*, 26(2), 107-114. <https://doi.org/10.12989/cac.2020.26.2.107>.
10. Hartmann, S., Weyler, R., Oliver J., Hernández, J. (2010). A 3D frictionless contact domain method for large deformation problems. *Computer Modeling in Engineering and Sciences (CMES)*, 55(3), 211-269. <https://doi.org/10.3970/cmcs.2010.055.211>.
11. Oliver, J., Hartmann, S., Cante, J., Weyler, R., Hernández, J. (2009). A contact domain method for large deformation frictional contact problems. Part 1: Theoretical basis. *Computer Methods in Applied Mechanics and Engineering*, 198, 2591-2606. <https://doi.org/10.1016/j.cma.2009.03.006>.
12. Chidlow, S.J., Chong, W.W.F., Teodorescu, M. (2013). On the two-dimensional solution of both adhesive and non-adhesive contact problems involving functionally graded materials. *European Journal of Mechanics-A/Solids*, 42(97), 136-140. <https://doi.org/10.1016/j.euromechsol.2012.10.008>.
13. Güler, M.A., Erdogan, F. (2004). Contact mechanics of graded coatings. *International Journal of Solids and Structures*, 41, 3865-3889. <https://doi.org/10.1016/j.ijsolstr.2004.02.025>.
14. El-Borgi, S., Abdelmoula, R., Keer, L. (2006). A receding contact plane problem between a functionally graded layer and a homogeneous substrate. *International Journal of Solids and Structures*, 43, 658-674. <https://doi.org/10.1016/j.ijsolstr.2009.06.008>.
15. Elloumi, R., Kallel-Kamoun, I., El-Borgi, S. (2010). A fully coupled partial slip contact problem in a graded half-plane. *Mechanics of Materials*, 42, 417-428. <https://doi.org/10.1016/j.mechmat.2010.01.002>.
16. Rekik, M., Neifar, M., El-Borgi, S. (2010). An axisymmetric problem of an embedded crack in a graded layer bonded to a homogeneous half-space. *International Journal of Solids and Structures*, 47, 2043-2055. <https://doi.org/10.1016/j.ijsolstr.2010.04.006>.

17. Nikbakht, A., Arezoodar, A.F., Sadighi, M., Zucchelli, A., Lari A.F. (2013). Frictionless elastic contact analysis of a functionally graded vitreous enameled low carbon steel plate and a rigid spherical indenter. *Composite Structures*, 96, 484-501. <https://doi.org/10.1016/j.compstruct.2012.08.044>.
18. Talezadehlari, A., Nikbakht, A., Sadighi, M., Zucchelli, A. (2016). Numerical analysis of frictional contact in the presence of a surface crack in a functionally graded coating substrate system. *International Journal of Mechanical Sciences*, 117, 286-298. <https://doi.org/10.1016/j.ijmecsci.2016.08.017>.
19. Kaya, Y. (2020). The contact problem of two layers one of Which is funtionally graded resting on a rigid plane and loaded by two rigid flat blocks. Ph.D. Dissertation; Institute of Natural Sciences, Karadeniz Technical University, Trabzon, Turkey.
20. Balcı, N.M., Dağ, S. (2019). Solution of the dynamic frictional contact problem between a functionally graded coating and a moving cylindrical punch. *International Journal of Solids and Structures*, 161, 267-281. <https://doi.org/10.1016/j.ijsolstr.2018.11.020>.
21. Polat, A. (2021). Examination of contact problem between functionally graded punch and functionally graded layer resting on elastic plane. *Structural Engineering and Mechanics*, 78(2), 135-143. <https://doi.org/10.12989/sem.2021.78.2.135>.
22. Polat, A., Kaya, Y., Kouider, B., Özşahin, T.Ş. (2019). Frictionless contact problem for a functionally graded layer loaded through two rigid punches using finite element method. *Journal of Mechanics*, 35(5), 591-600. <https://doi.org/10.1017/jmech.2018.55>.
23. Yan, J., Mi, C. (2020). On the receding contact between a homogeneous elastic layer and a half-plane substrate coated with functionally graded materials. *International Journal of Computational Methods*, 17(1), 1-21, <https://doi.org/10.1142/S0219876218440085>.
24. Kaya, Y., Polat, A., Özşahin, T.Ş. (2020). Analytical and finite element solutions of continuous contact problem in functionally graded layer. *The European Physical Journal Plus*, 135(1), 1-21. <https://doi.org/10.1140/epjp/s13360-020-00138-9>.
25. Öner, E., Birinci, A. (2020). Investigation of the solution for discontinuous contact problem between a functionally graded (FG) layer and homogeneous half-space. *Archive of Applied Mechanics*, 90, 18-19. <https://doi.org/10.1007/s00419-020-01750-y>.
26. Polat, A., Kaya, Y. (2022). Analysis of discontinuous contact problem in two functionally graded layers resting on a rigid plane by using finite element method. *Computers and Concrete*, 29(4), 247-253. <https://doi.org/10.12989/cac.2022.29.4.247>.
27. Erdogan, F., Gupta, G. (1972). On the numerical solution of singular integral equations. *Quarterly of Applied Mathematics*, 29, 525-534. <https://doi.org/10.1090/QAM/408277>.
28. Polat, A. (2019). Contact Problem of Functionally Graded Layer Loaded by Two Rigid Stamps and Resting on an Elastic Half Plane. Ph.D. Dissertation; Institute of Natural Sciences Karadeniz Technical University, Trabzon, Turkey.
29. Bora, P. (2016). The contact problem for two elastic layers loaded by means of two rigid rectangle blocks and resting on an elastic half infinite plan. Ph.D. Dissertation; Institute of Natural Sciences Karadeniz Technical University, Trabzon, Turkey.
30. Yaylaci, M., Adıyaman, G., Oner, E., Birinci, A. (2021). Investigation of continuous and discontinuous contact cases in the contact mechanics of graded materials using analytical method and FEM. *Computers and Concrete*, 27(3), 199-210. <https://doi.org/10.12989/cac.2021.27.3.199>.